Achromatic Liquid Crystals Variable Retarders Preliminary Study Report

Capobianco G. , Fineschi S.

Report nr. 124 date: 28/10/2009

Achromatic Liquid Crystals Variable Retarders Preliminary Study Report

Authors: G. Capobianco, S. Fineschi
Date: 28 October 2009

INDEX

DOCUMENT CHANGE RECORD

REV	DESCRIPTION OF CHANGE	PROVIDED BY	INPUT DATE
0.0	OATo Technical Report nr.124	G. Capobianco	28 Oct. 2009

1. MATERIALS

For this simulation we use two liquid crystals (LCs):

- Merck E7

- Merck ZLI-1132

E7	Ternary eutectic mixture of 47% 5CB (pentylcyanobiphenyl), 25% 7CB (heptyloxycyanobiphenyl), 18% 8OCB (octyloxycyanobiphenyl), and 10% T15
ZLI 1132	Mixture of three trans-4-alkyl-(4-cyanophenyl)cyclohexanes with propyl, pentyl, and heptyl as the alkyl groups and trans-4-pentyl-(4′-cyanobiphenyl-4)cyclohexane 24/36/25:15

2. MODELS for BIREFRINGENCE DISPERSION

The single-band model describes the LC birefringence as a function of wavelength:

$$\Delta n = G \cdot \frac{\lambda^2 \cdot \lambda_0^2}{\lambda^2 - \lambda_0^2} \qquad (1)$$

In the Cauchy model, the ordinary and extraordinary indices are approximated by:

$$n_{e,o} = A_{e,o} + \frac{B_{e,o}}{\lambda^2} + \frac{C_{e,o}}{\lambda^4} \qquad (2)$$

The birefringence is:

$$\boldsymbol{\Delta n \equiv n_e - n_o} \qquad (3)$$

2.1 MERCK-E7

With the single-band birefringence dispersion model (Eq. 1), and the coefficient listed in [1]:

$$\begin{cases} G = 3.06 \cdot 10^{-6} [nm^{-2}] \\ \lambda_0 = 250 [nm] \end{cases} \qquad (4)$$

the resulting birefringence vs. wavelength, in the range 450-650 nm, is shown in Fig.1:

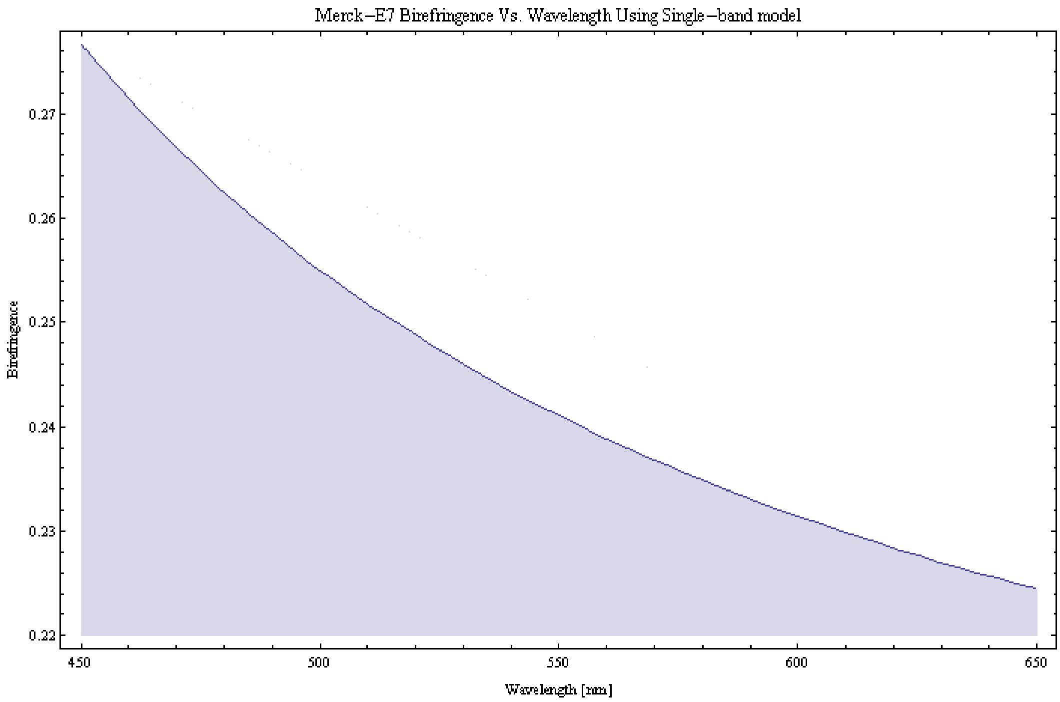

Figure 1 – Merck-E7 Birefringence vs. Wavelength (single-band dispersion model)

The birefringence value of 0.225 provided by ARCOPTIX is obtained for λ = 645nm. This same value of birefringence is reported in [2] for T=20C and λ =589 nm. The parameters G and λ_0 used for this simulation are probably obtained for T=23 °C (G is temperature-dependent).

Figure 3 shows the data from [3] at T = 23 °C for the ordinary and extraordinary refractive indices.

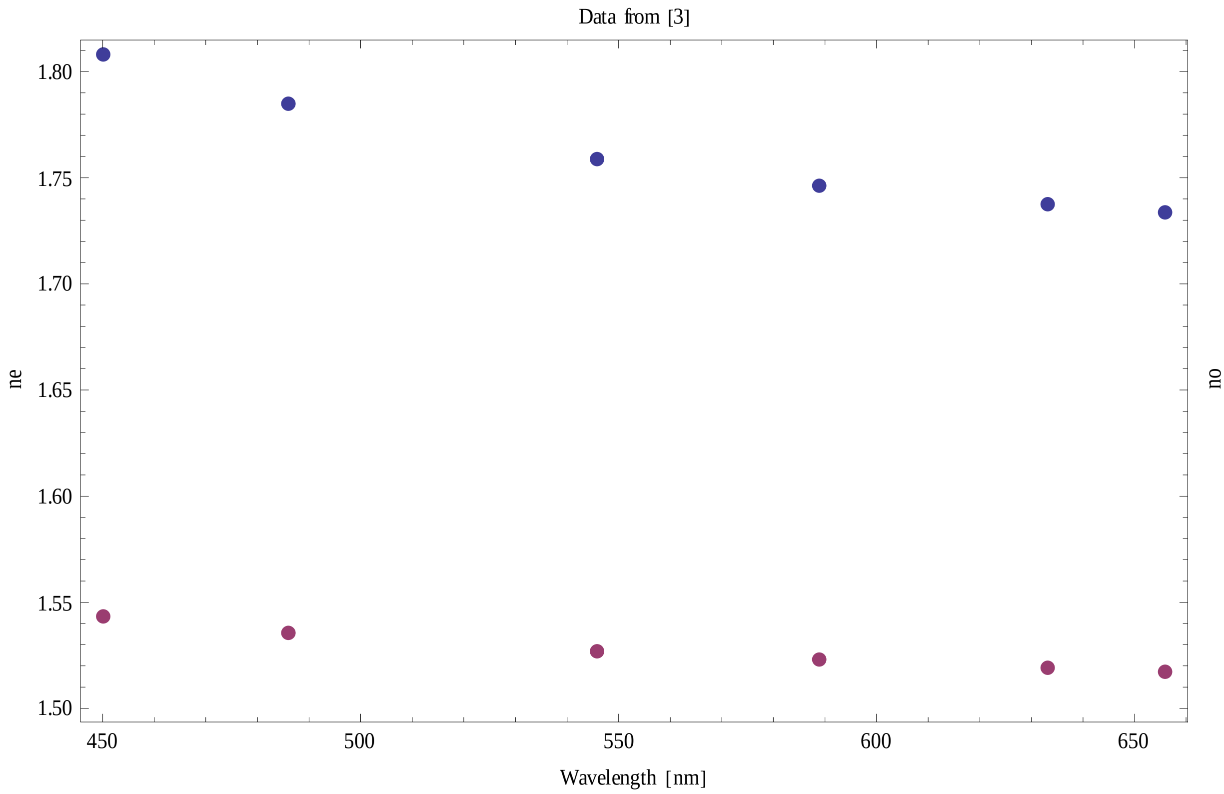

Figure 2 – Merck-E7 ordinary and extraordinary refractive indices data from [3]

Figure 3 shows the birefringence vs. wavelength resulting from the data of the ordinary and extraordinary refractive indices:

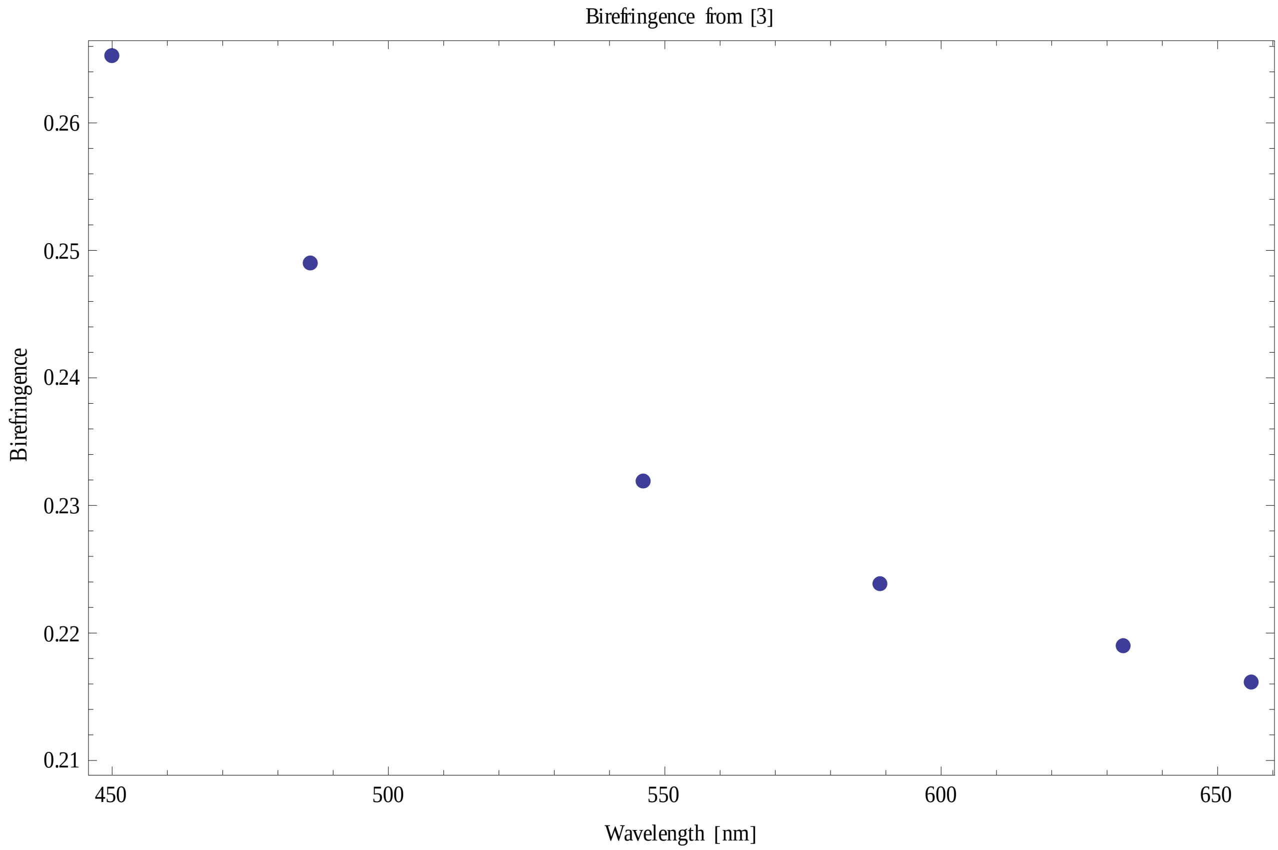

Figure 3 – Merck-E7 birefringence. Data from [3]

The Cauchy parameters derived from fitting these data are:

$$
\begin{aligned}
A_e &= 1.6985\\
B_e &= 8956.69\ \mathrm{nm}^{-2}\\
C_e &= 2.69175\times10^{9}\ \mathrm{nm}^{-4}\\
A_o &= 1.49949\\
B_o &= 6830.58\ \mathrm{nm}^{-2}\\
C_o &= 4.05656\times10^{8}\ \mathrm{nm}^{-4}
\end{aligned}
\qquad (5)
$$

Figure 4 shows the resulting fits.

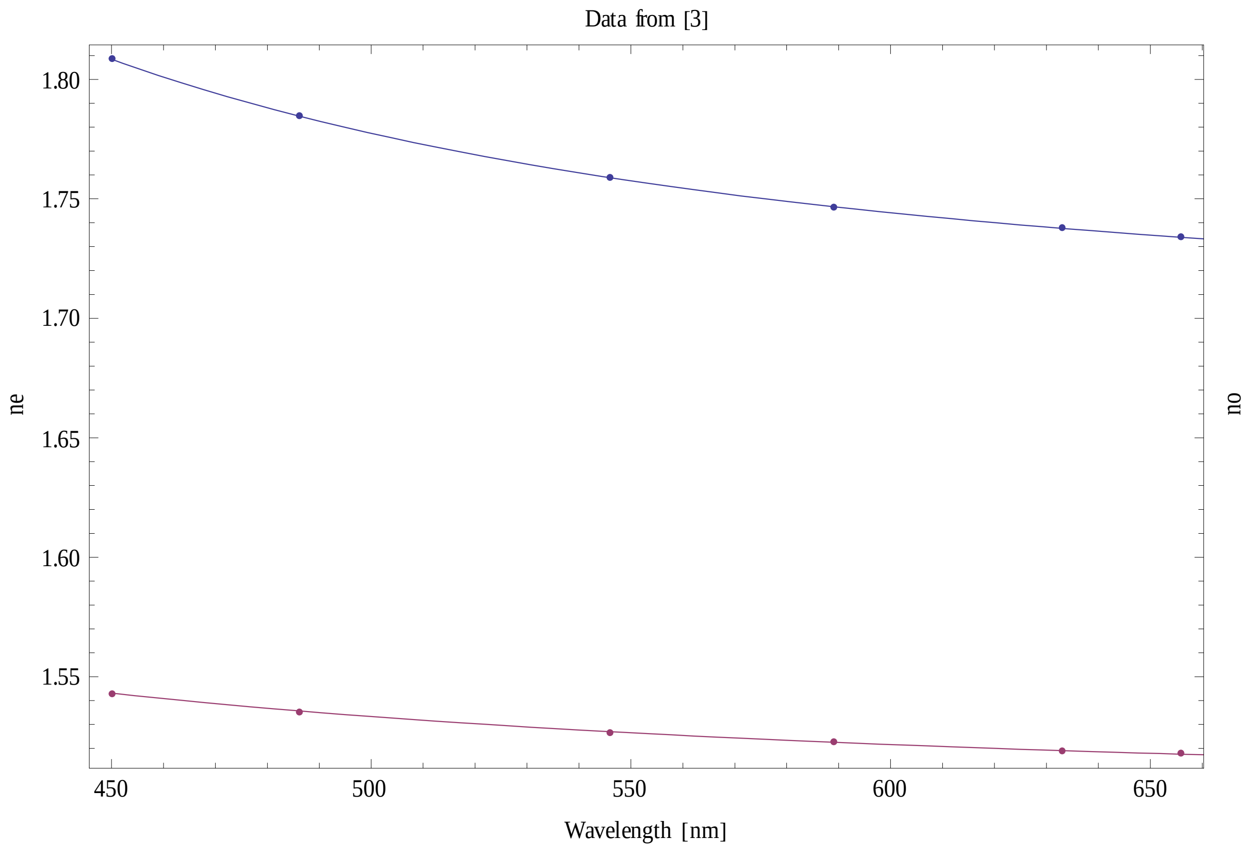

Figure 4 – Merck-E7. Fits with the 3-coefficients Cauchy Model of the ordinary and extraordinary refractive indices

Figure 5 shows the birefringence derived from the fitted data with Eq. 3

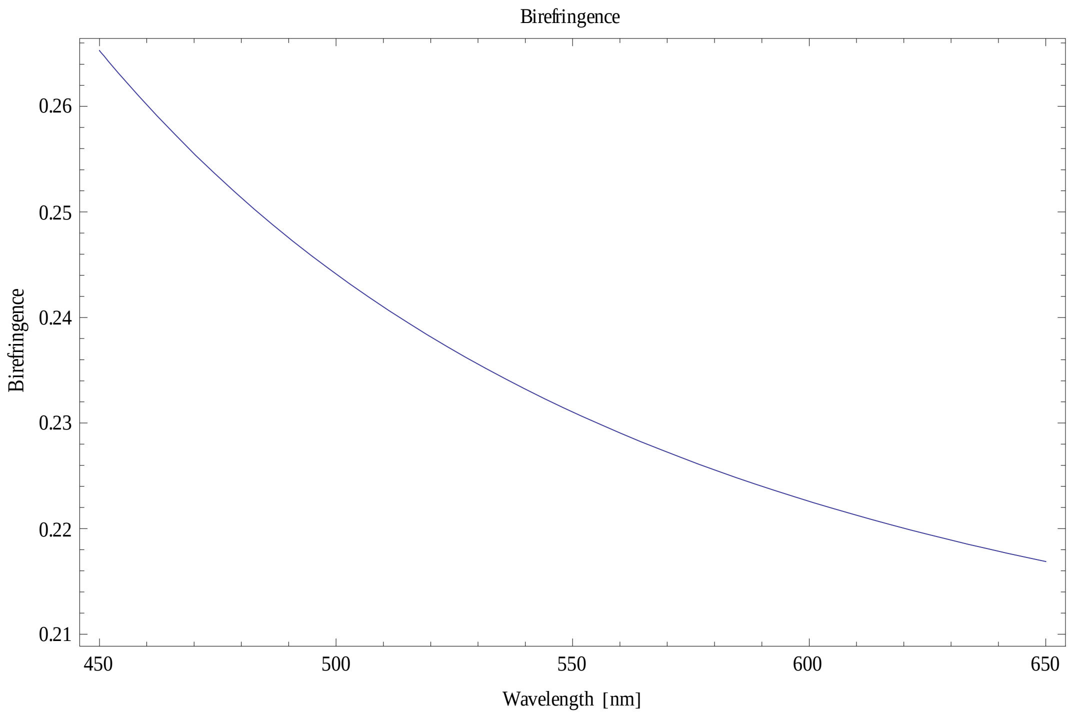

Figure 5 – Merck-E7. Birefringence using 3-coefficients Cauchy Model

According to [2], the birefringence is 0.225 at 584 nm. Fitting this curve with a single-band dispersion model (Eq. 1), we obtain [FitA]:

$$\begin{cases} G = 3.038 \cdot 10^{-6} [nm^{-2}] \\ \lambda_0 = 246.8 [nm] \end{cases} \qquad (6)$$

Setting $\lambda_0 = 250$ nm, we obtain: $G = 2.94 \cdot 10^{-6} [nm^{-2}]$ [FitB].

Figure 6 shows [FitA], [FitB] and difference between n_e and n_o [FitC].

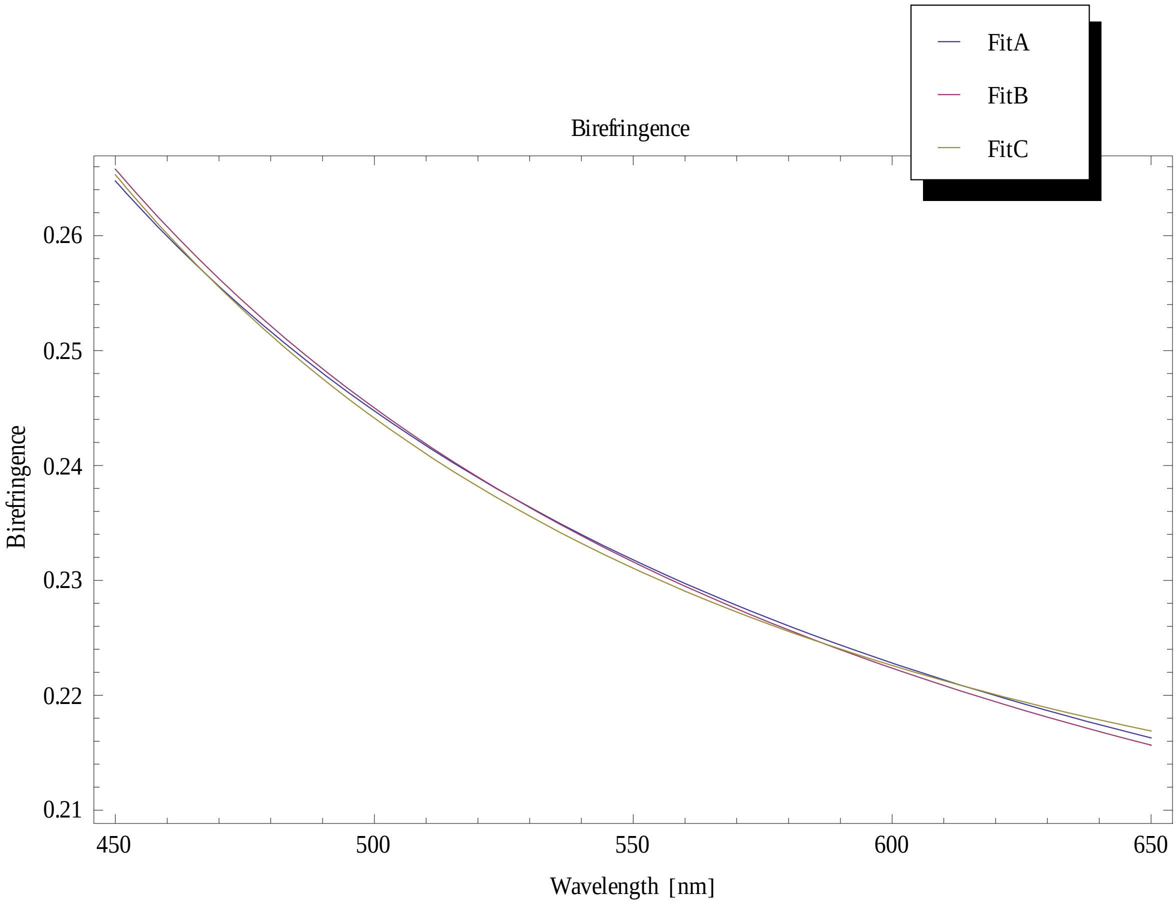

Figure 6 – Merck-E7. Birefringences from the single-band model compared to that from the Cauchy model

Introducing the coefficients derived from the fits (Eqs. 5) in the Cauchy model (Eq. 4), the expression for the birefringence dispersion is:

$$\Delta n(\lambda) = n_e - n_o = A_e - A_o + \frac{B_e - B_o}{\lambda^2} + \frac{C_e - C_o}{\lambda^4} = 0.19904 + \frac{2126.11}{\lambda^2} + \frac{2.28609 \cdot 10^9}{\lambda^4}$$

$$n_o(\lambda) = 1.4995 + \frac{6830.58}{\lambda^2} + \frac{4.05656 \cdot 10^8}{\lambda^4} \qquad (7)$$

2.2 MERCK ZLI-1132

Bibliography on this Nematic Liquid Crystal is not as extensive as for E7.

The parameters for the single-band dispersion model are [1]:

$$\begin{cases} G = 3.15 \cdot 10^{-6} [nm^{-2}] \\ \lambda_0 = 198 [nm] \end{cases} \quad (8)$$

The birefringence value of 0.1396, found at 589 nm in [2], is obtained at 583 nm with these parameters.

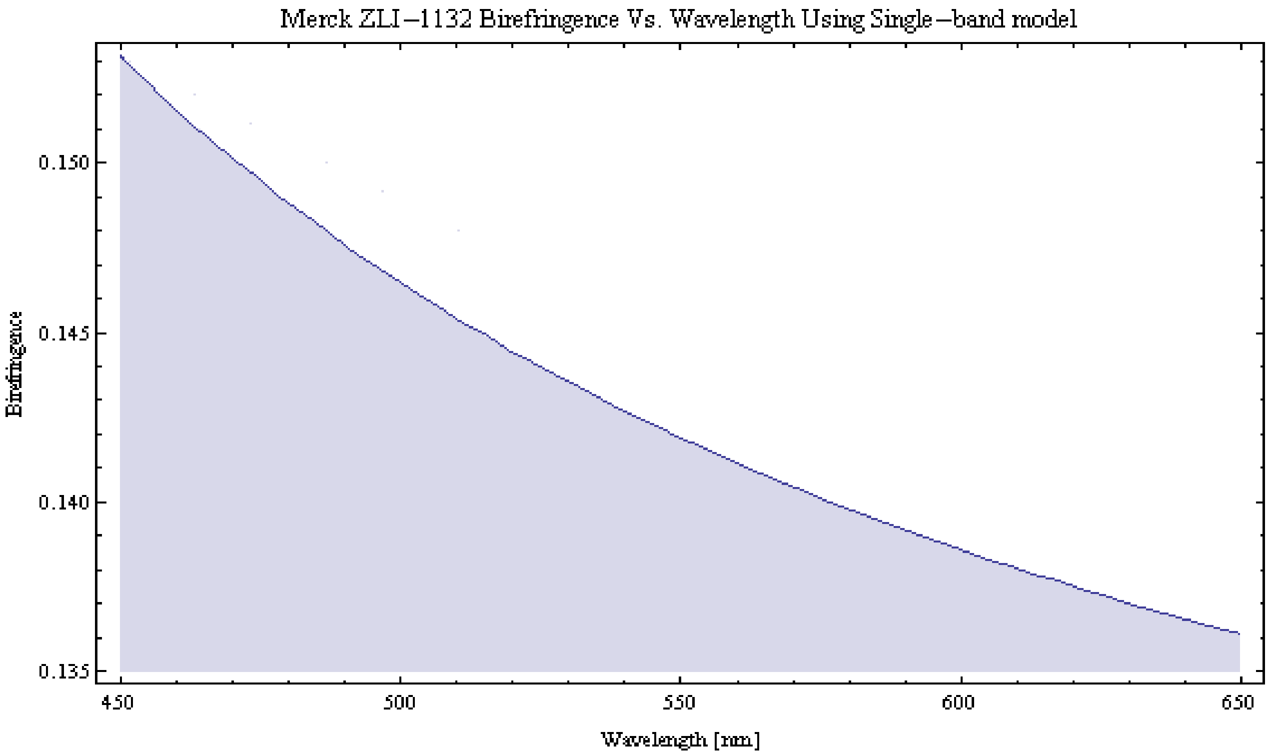

Figure 7 – Merck ZLI-1132 Birefringence vs. Wavelength using Single-band dispersion model

From the data in [4], the ordinary and extraordinary refractive indices are:

$A_e = 1.3758$

$B_e = 138122\ nm^{-2}$

$C_e = -1.73186\times10^{10}\ nm^{-4}$ (9)

$A_o = 1.26867$

$B_o = 125866\ nm^{-2}$

$C_o = -1.6666\times10^{10}\ nm^{-4}$

Figure 8 and 9 show the ordinary and extraordinary refractive indices and the birefringence, respectively:

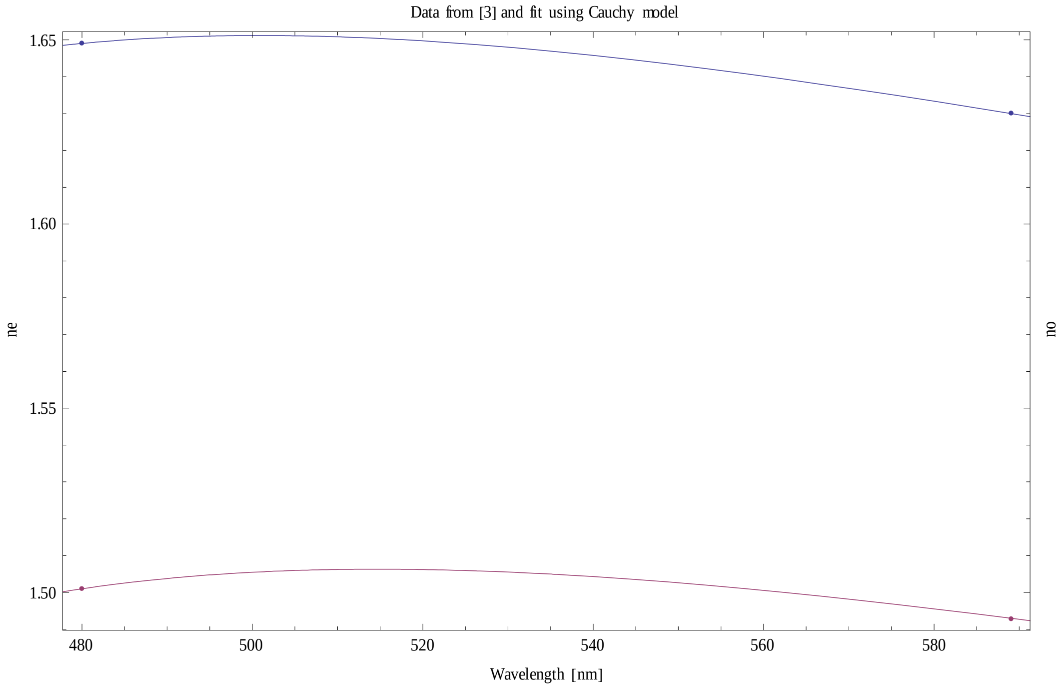

Figure 8 – Merck ZLI-1132. Fits with the 3-coefficients Cauchy Model of the ordinary and extraordinary refractive indices

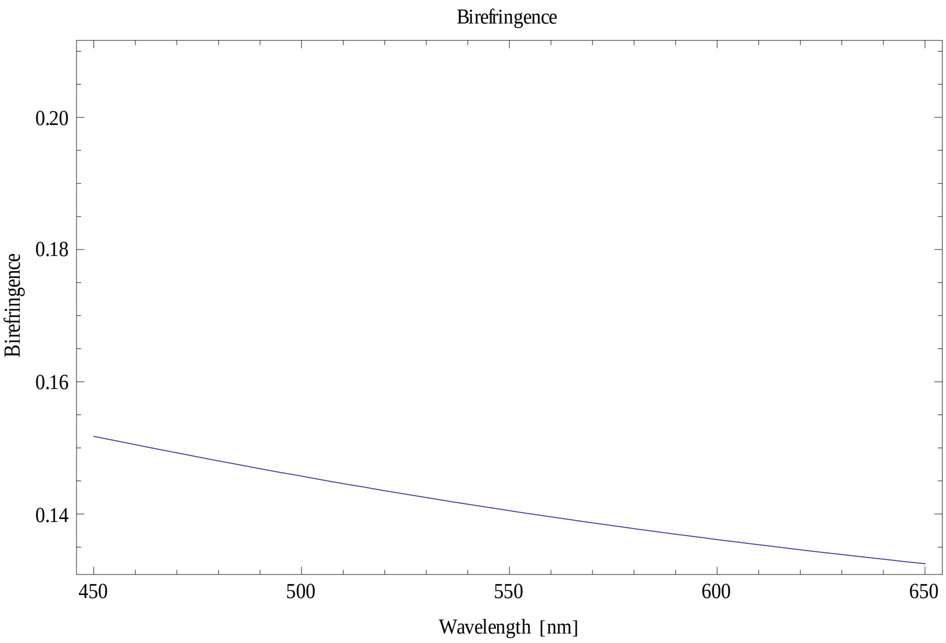

Figure 9 – Merck ZLI-1132. Birefringence with the Cauchy Model

The fit with single-band dispersion model (1), gives the parameters: [FitA]

$$\begin{cases} G = 2.688 \cdot 10^{-6} [nm^{-2}] \\ \lambda_0 = 210.815 [nm] \end{cases} \quad (10)$$

If $\lambda_0 = 198$ nm, then: $G = 3.12 \cdot 10^{-6} [nm^{-2}]$ [FitB].

Figure 10 compares the single-band [FitA], [FitB] and Cauchy models [FitC].

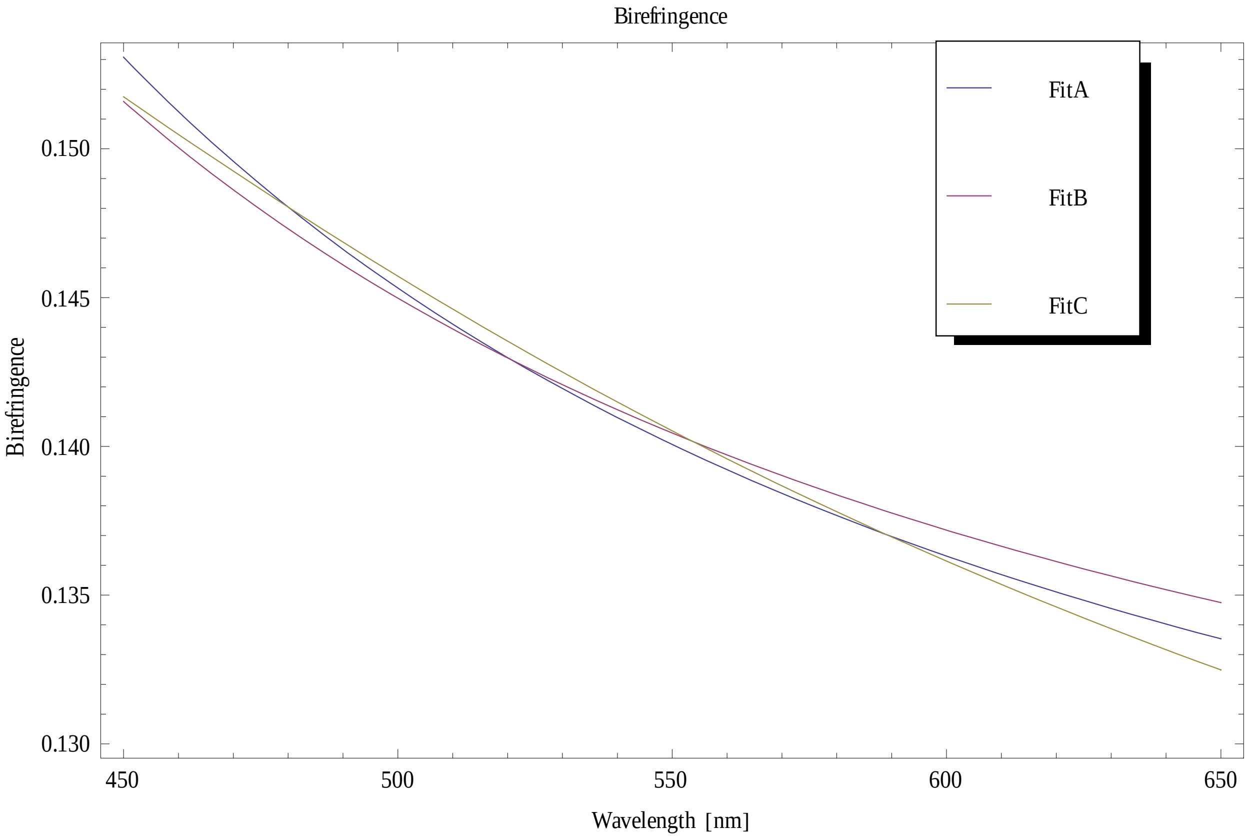

Figure 10 – Merck ZLI-1132. Birefringence from single-band [FitA], [FitB] and Cauchy [FitC]s models

Introducing the coefficients derived from the fits (Eqs. 9) in the Cauchy model (Eq. 4), the expression for the birefringence dispersion is:

$$\Delta n(\lambda) = n_e - n_o = A_e - A_o + \frac{B_e - B_o}{\lambda^2} + \frac{C_e - C_o}{\lambda^4} = 0.10713 + \frac{12256}{\lambda^2} - \frac{6.521 \cdot 10^8}{\lambda^4}$$

$$n_o(\lambda) = 1.26867 + \frac{125866}{\lambda^2} - \frac{1.66665 \cdot 10^{10}}{\lambda^4} \quad (11)$$

3. ACHROMATIC LC PLATE WITH FIXED HALF-WAVE RETARDATION

If two LC layers are oriented with the molecules pointing in orthogonal directions then the retardance of the 2 layers subtracts. The overall retardance is determined by the difference in thickness between the two LC layers. By using two different LC materials, with different dispersions, the thickness of the layers can be adjusted while keeping the retardance difference fixed, so that the net retardance is wavelength insensitive. This is known as **"dispersion balancing"**:

$$\Delta \boldsymbol{n}_{LC1}(\lambda_i)\cdot \boldsymbol{d}_{LC1} - \Delta \boldsymbol{n}_{LC2}(\lambda_i)\cdot \boldsymbol{d}_{LC2} = \lambda_i \cdot \rho \quad (\boldsymbol{i} = \boldsymbol{a},\boldsymbol{b}) \qquad (12)$$

where $\boldsymbol{d}_{LC1}, \boldsymbol{d}_{LC2}$ are the thicknesses of the first and second LC layer, and λ_i $(\boldsymbol{i} = \boldsymbol{a},\boldsymbol{b})$ the wavelength range where the retardance, ρ, is achromatic.

As an example of dispersion balancing, we use the Cauchy models (Eqs. 7, 11) of the birefringence vs. wavelength of the E7 and ZLI-1132 LCs and combine them to obtain a LC wave-plate with fixed half-wave retardance: $\rho = 1/2$. Figure 11 and 12 show the birefringence and the ordinary indices of those LCs materials, respectively.

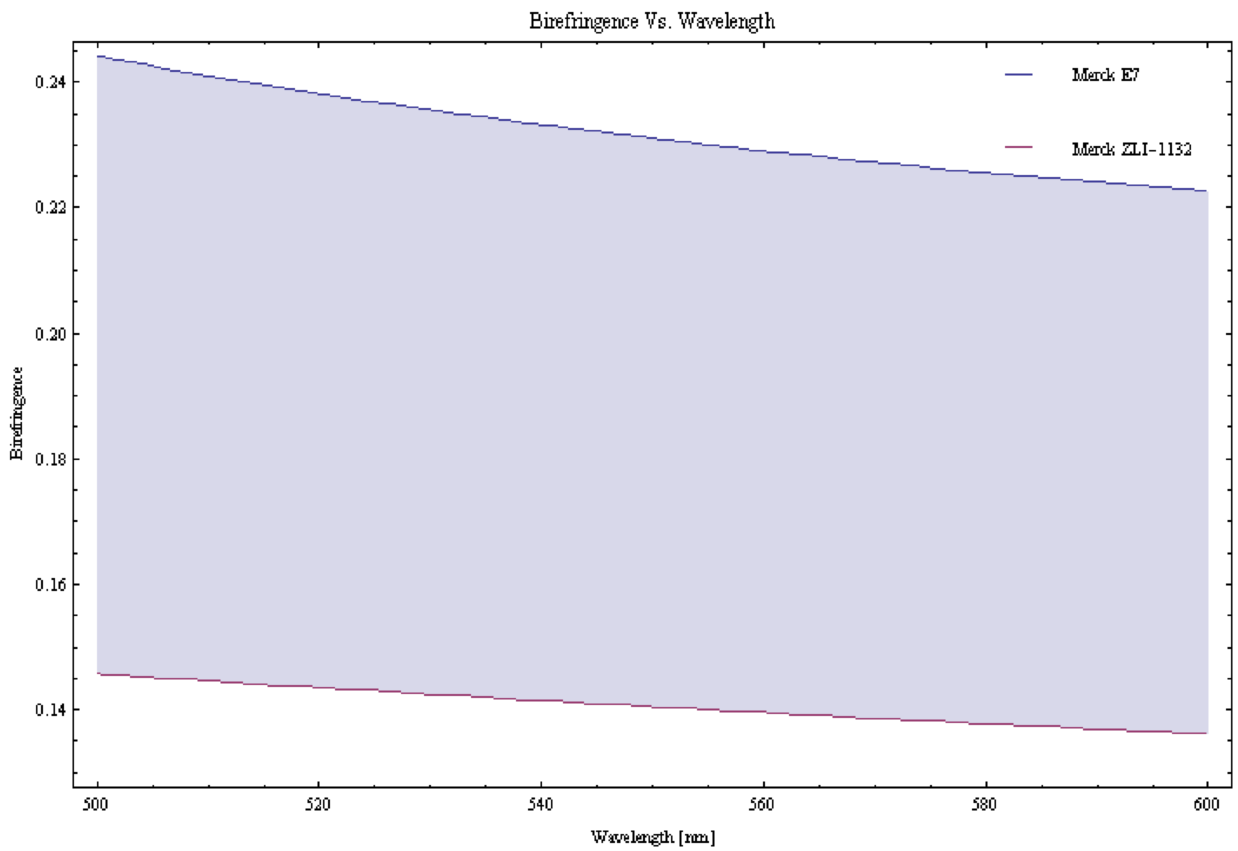

Figure 11 –Birefringence vs. Wavelength for the selected LCs

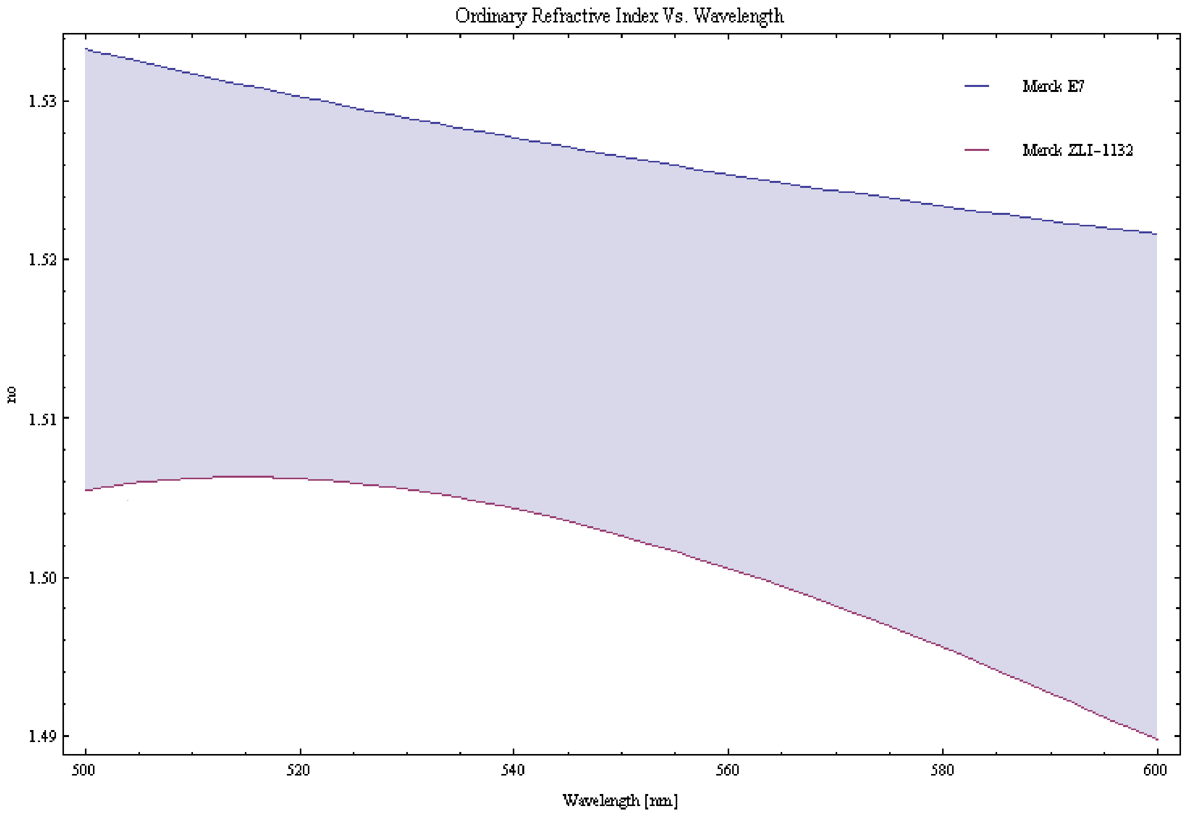

Figure 12 –Ordinary refractive index (no) vs. Wavelength for the selected LCs

We optimize the achromaticity of the LC half-plate retarder by varying the LCs layers thicknesses and wavelength ranges with three different cases:

Case #1:

$\lambda_a = 500\,\text{nm};\ \lambda_b = 600\,\text{nm}$

$d_{LC1} = 12097.5\,\text{nm};\ d_{LC2} = 21982\,\text{nm}$

Case #2:

$\lambda_a = 530\,\text{nm};\ \lambda_b = 570\,\text{nm}$

$d_{LC1} = 13404\,\text{nm};\ d_{LC2} = 24019\,\text{nm}$

Case #3:

$\lambda_a = 515\,\text{nm};\ \lambda_b = 585\,\text{nm}$

$d_{LC1} = 12865\,\text{nm};\ d_{LC2} = 23179\,\text{nm}$

These three cases are showed in Fig.13. Case#2 minimizes the area in the graph with half-wave retardance.

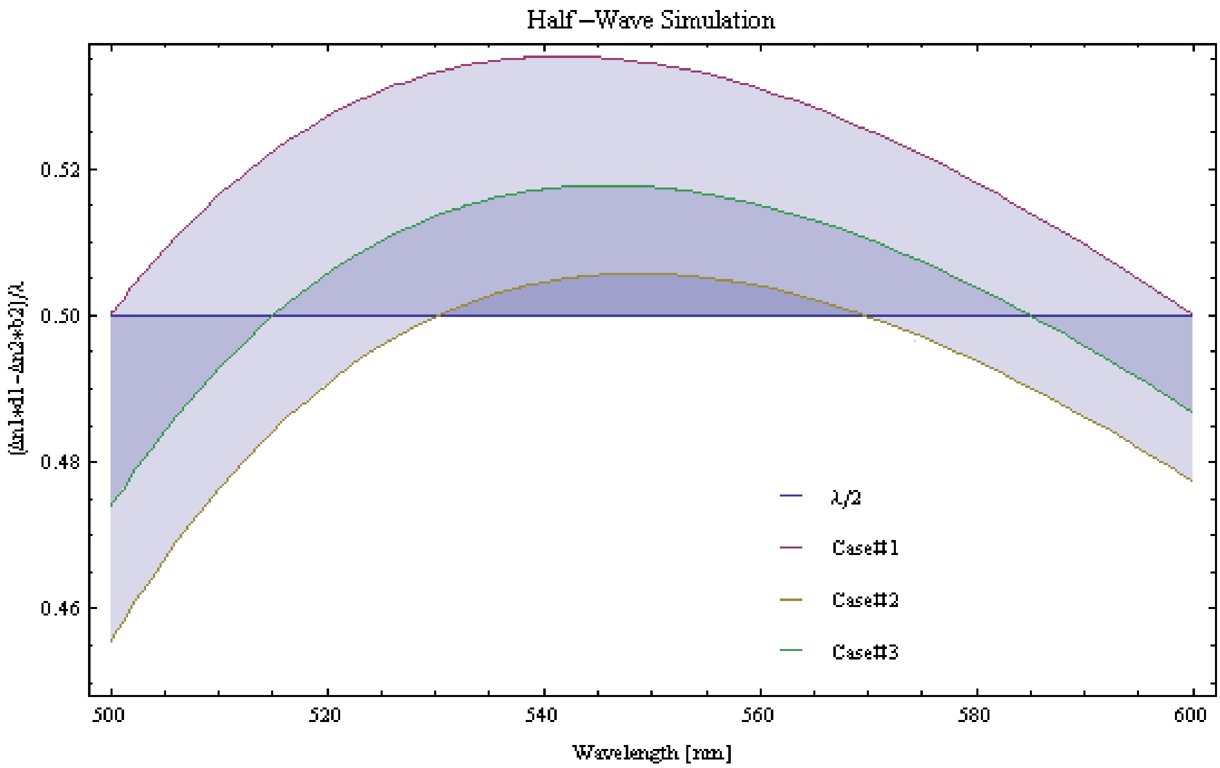

Figure 13 –Half Wave Simulation using theoretical thickness

The LCs thicknesses commercially available to ARCOPTIX are: 4.5, 6.5, 7.5, 10, 20 and 100 µm. The thicknesses closest to the theoretical ones are 10 and 20 µm for E7 and ZLI-1132, respectively. The resulting retardance vs. wavelength is plotted in Fig.14. In the [500, 600] nm range, the average retardance is 0.9 wave.

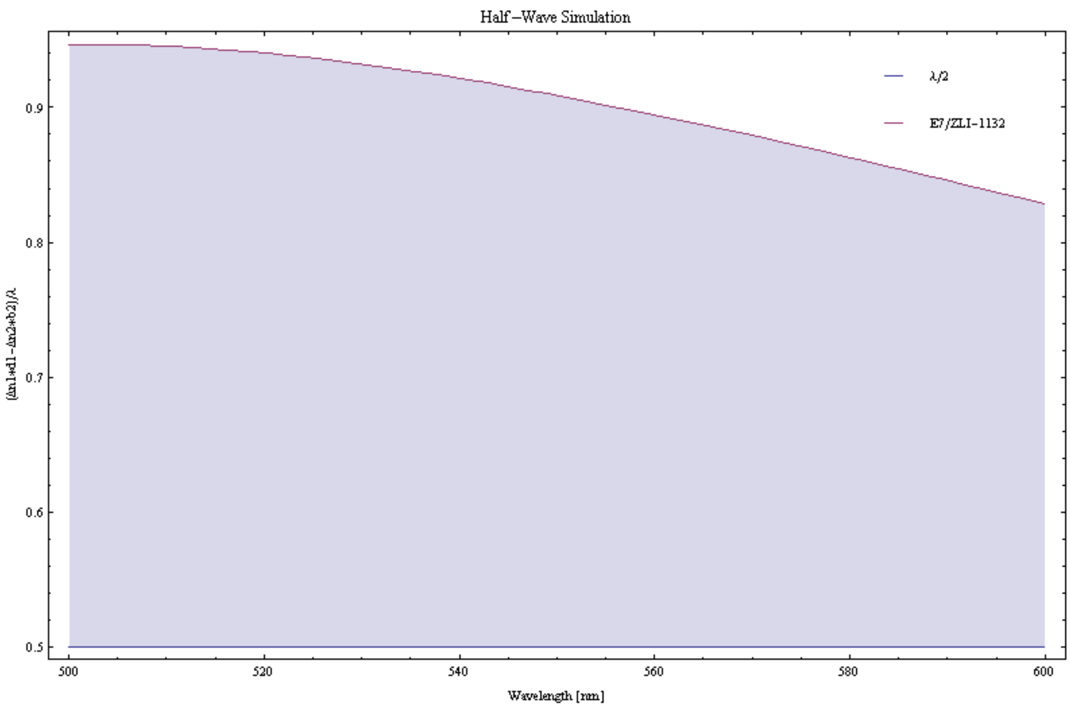

Figure 14 –Dispersion balancing simulation using commercial thickness.

Using thickness of 4.5 and 10 μm for E7 and ZLI-1132 respectively, we obtain retardance showed in fig. 15. Average retardance is 0.65 waves.

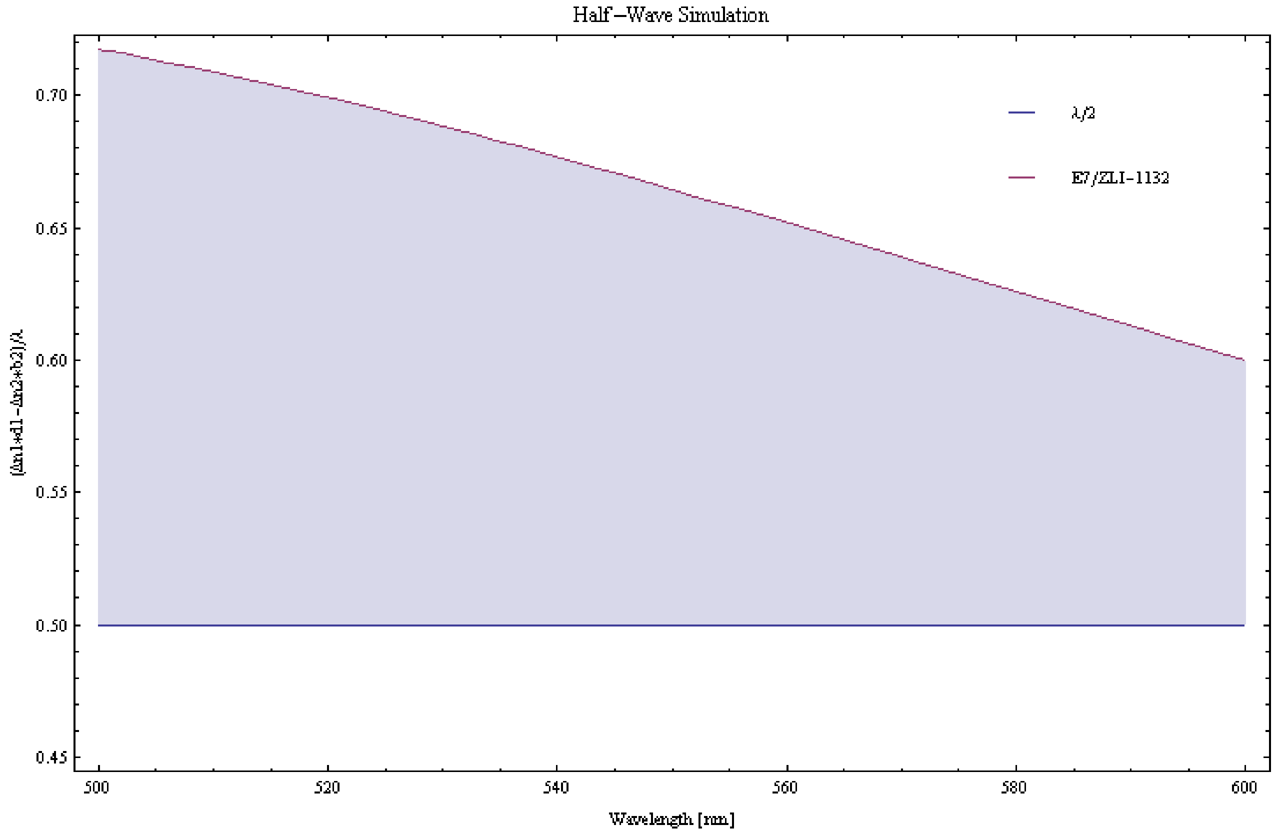

Figure 15 –Dispersion balancing simulation using commercial thicknesses of 4.5 (E7) and 10 μm (ZLI-1132).

4. ACHROMATIC LC VARIABLE RETARDER

We extend the approach of dispersion balancing to combine two LC layers that result in an achromatic response for different retardances in a given wavelength range. In order for the LC pair to be achromatic and tunable within a given retardance and wavelength range, the dispersion balancing (Eq. 12) should be maintained for different tilt angles, ϑ, of the LC molecules about the optical axis.

The effective retardance variation, $\bar{\rho}$, vs. tilt angle and wavelength is given by:

$$\lambda \cdot \bar{\rho}(\vartheta) = \Delta\bar{\boldsymbol{n}}(\lambda,\vartheta)\cdot \boldsymbol{d} \qquad (13)$$

where the effective birefringence, $\Delta\bar{\boldsymbol{n}}$, is given by: [6, 7]

$$\Delta\bar{\boldsymbol{n}}(\lambda,\vartheta) = \left[\frac{\boldsymbol{n_o}+\Delta\boldsymbol{n}}{\sqrt{1+\left(\frac{2\Delta\boldsymbol{n}}{\boldsymbol{n_o}}+\frac{\Delta\boldsymbol{n}^2}{\boldsymbol{n_o}^2}\right)\cdot\sin^2(\vartheta)}}-\boldsymbol{n_o}\right] \approx \Delta\boldsymbol{n}\ (1-\sin^2\vartheta) - \frac{3}{8}\frac{\Delta\boldsymbol{n}^2}{\boldsymbol{n_o}}\sin^2 2\vartheta \qquad (14)$$

Plots of the effective retardances for E7 and ZLI-1132 as a function of wavelength and tilt angle are shown in Fig. 16.

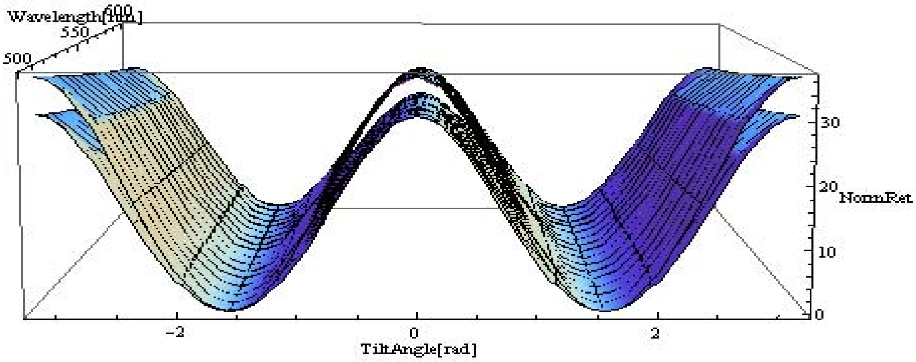

Figure 16 – Retardances as a function of wavelength and tilt angle for E7 (upper surface) and ZLI-1132 (lower).

Given the wavelength range [λ_a, λ_b] = [*500, 600*] nm, and the retardance range [$\bar{\rho}_0, \bar{\rho}_1$] = [*0, 3/4*] λ, the extremes of the tilt angles range [ϑ_0, ϑ_1], and the thicknesses, d_{LC1}, d_{LC2} , of the two-layer tunable LC are derived by solving the four dispersion-balancing equations in four unknowns (ϑ_0, ϑ_1 and $\boldsymbol{d_{LC1}}$, $\boldsymbol{d_{LC2}}$):

$$\Delta\bar{\boldsymbol{n}}_{LC1}(\lambda_i,\vartheta_0)\cdot \boldsymbol{d}_{LC1} - \Delta\bar{\boldsymbol{n}}_{LC2}(\lambda_{,i},\vartheta_0)\cdot \boldsymbol{d}_{LC2} = \lambda_i \cdot \bar{\rho}_0(\vartheta_0) \quad (\boldsymbol{i}=\boldsymbol{a},\boldsymbol{b})$$

(15)

$$\Delta\bar{\boldsymbol{n}}_{LC1}(\lambda_i,\vartheta_1)\cdot \boldsymbol{d}_{LC1} - \Delta\bar{\boldsymbol{n}}_{LC2}(\lambda_{,i},\vartheta_1)\cdot \boldsymbol{d}_{LC2} = \lambda_i \cdot \bar{\rho}_1(\vartheta_1) \quad (\boldsymbol{i}=\boldsymbol{a},\boldsymbol{b})$$

Zero-retardance is achieved for $\vartheta_0 = \pi/2$ (i.e., high bias voltages):

$$\Delta\bar{\boldsymbol{n}}_{LC1}(\lambda_i,0)\cdot \boldsymbol{d}_{LC1} - \Delta\bar{\boldsymbol{n}}_{LC2}(\lambda_{,i},0)\cdot \boldsymbol{d}_{LC2} = 0 \quad (\boldsymbol{i}=\boldsymbol{a},\boldsymbol{b}) \qquad (16)$$

The approach to design an achromatic LC variable retarder (ALCVR) entails two steps:

1) The thicknesses of the two LC layers are derived by first setting $\vartheta_1 = 0$ (i.e., low bias voltages) and solving the dispersion-balancing equations for the 3/4-wave retardance. In this

case, the dispersion-balancing equations reduce to those with the standard (i.e., not effective) ordinary and extraordinary indices:

$$\Delta n_{LC1}(\lambda_i)\cdot d_{LC1} - \Delta n_{LC2}(\lambda_{,i})\cdot d_{LC2} = \lambda_i \cdot 3/4 \quad (i = a,b) \tag{17}$$

We optimize the achromaticity of the LC 3/4-wave plate retarder by varying the LCs layers thicknesses and wavelength ranges with three different cases:

Case #1:

$\lambda_a = 500\,\text{nm};\ \lambda_b = 600\,\text{nm}$

$d_{LC1} = 18146\,\text{nm};\ d_{LC2} = 32973\,\text{nm}$

Case #2:

$\lambda_a = 530\,\text{nm};\ \lambda_b = 570\,\text{nm}$

$d_{LC1} = 20105\,\text{nm};\ d_{LC2} = 36029\,\text{nm}$

Case #3:

$\lambda_a = 515\,\text{nm};\ \lambda_b = 585\,\text{nm}$

$d_{LC1} = 19298\,\text{nm};\ d_{LC2} = 34769\,\text{nm}$

These three cases are showed in Fig.17. Case#2 minimizes the area in the graph with 0.75-wave retardance.

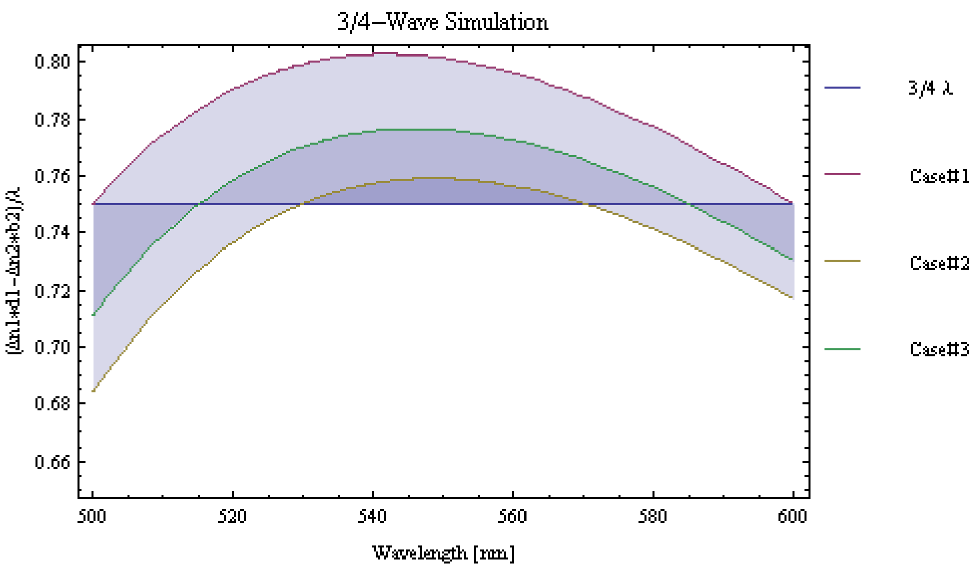

Figure 17 –3/4-Wave Simulation using theoretical thickness

Then wave plates thicknesses are 20 μm for E7 and 36 μm for ZLI-1132. Using this thicknesses, we obtain (Fig. 18):

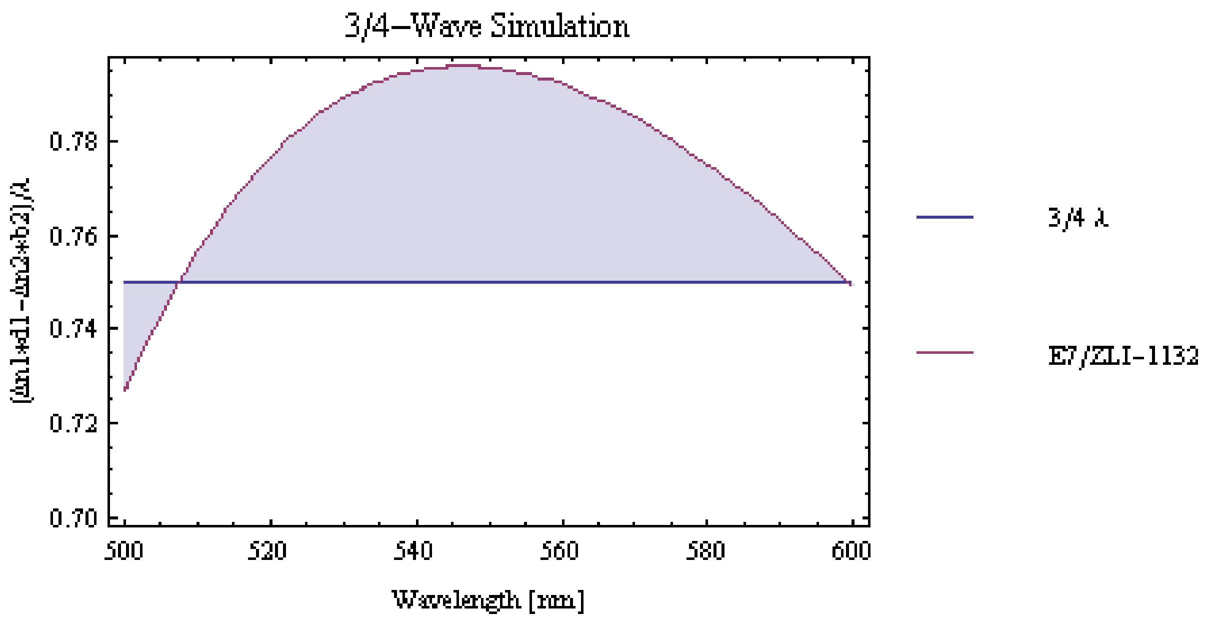

Figure 18 -3/4-Wave Simulation using thicknesses of 20 μm for E7 and 36 μm for ZLI-1132

Using commercial thicknesses of 20 and 100 μm, we obtain (fig.18a):

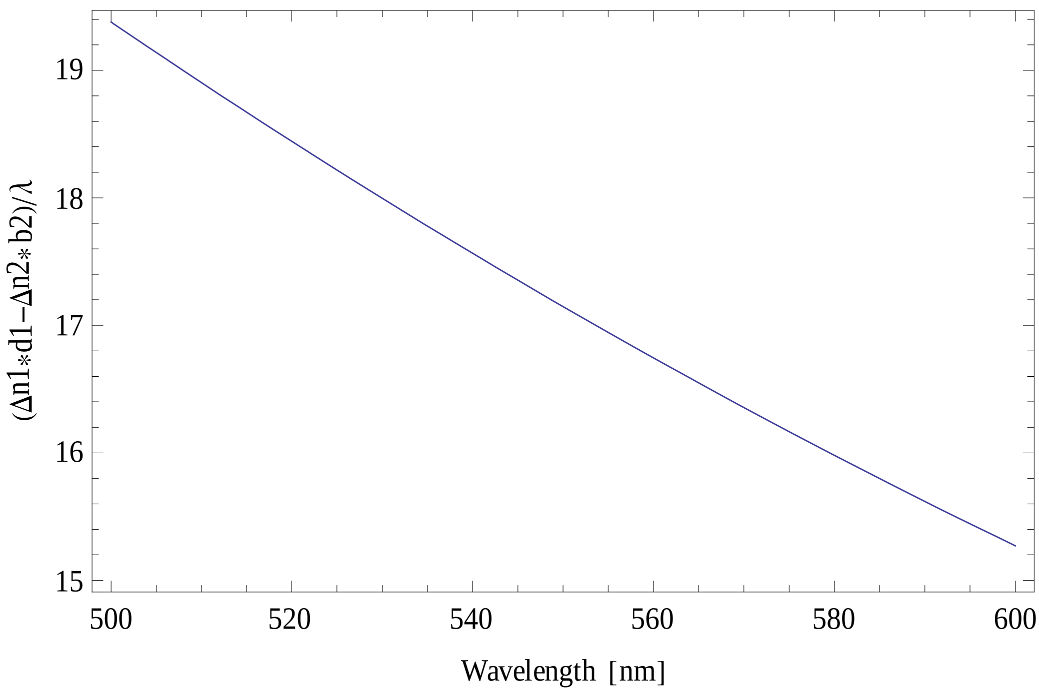

Figure 18a- Variable Retarder Simulation using thicknesses of 20 μm for E7 and 100 μm for ZLI-1132

2) Then, the tilt angles are varied within the range $0 < \vartheta < \pi/2$, and the achromaticity of the effective retardances is verified as the latter vary within the range $0 < \overline{\rho}(\vartheta) < 3/4$, in the dispersion-balancing equations (15) .

Plot of effective retardance vs. wavelength for different tilt angle values for 2 materials is in fig. 19. Materials used for this simulation are:

- E7 (thickness: 20μm);
- ZLI-1132 (thickness: 36μm).

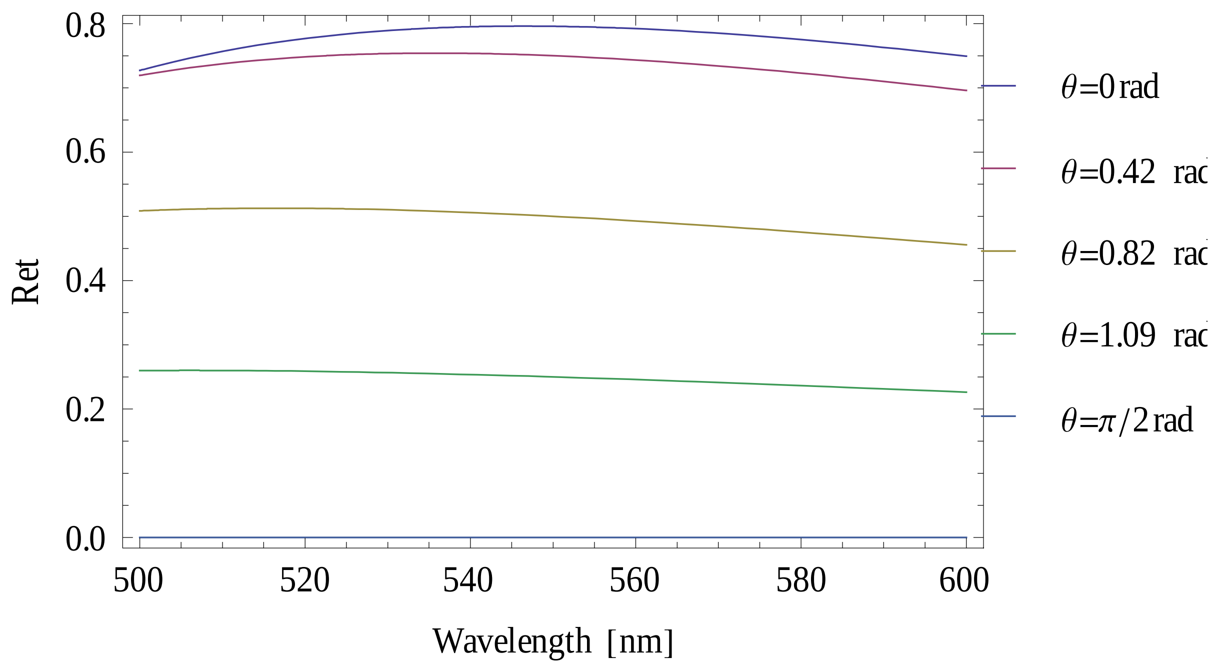

Figure 19 –Plot of effective retardance vs. wavelength (thicknesses: 20μm, 36μm)

Using proposed thickness of 10 and 20 μm, plot is the follow (fig.20).

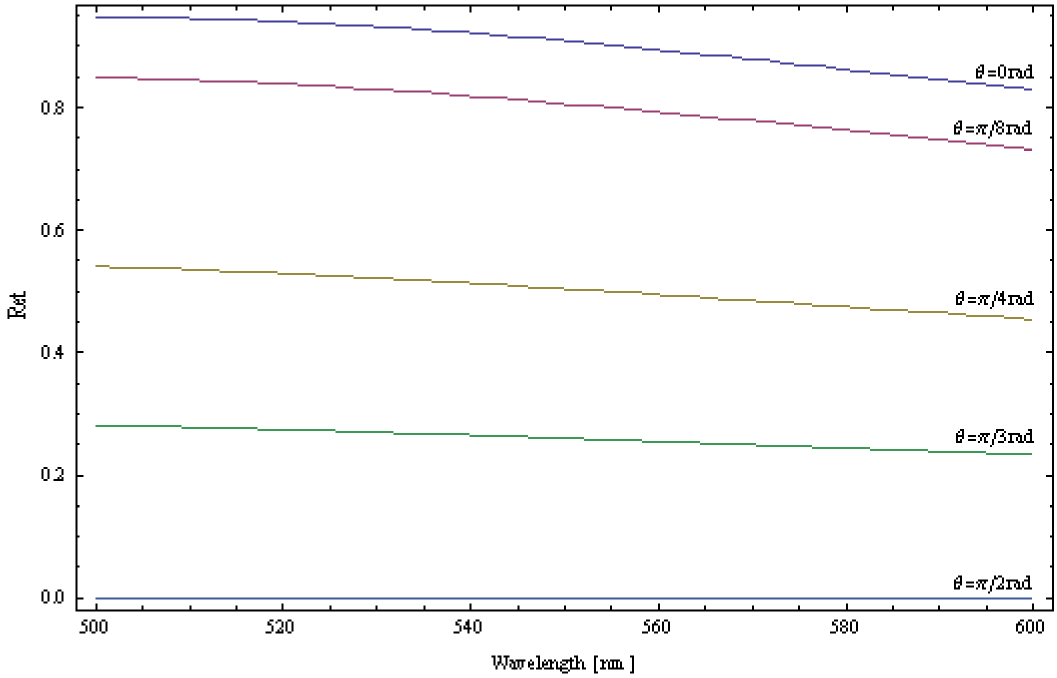

Figure 20 –Plot of effective retardance vs. wavelength for thicknesses of 10 and 20 μm

Using commercial thicknesses of 20 and 100 μm, retardance is the follow (fig. 21):

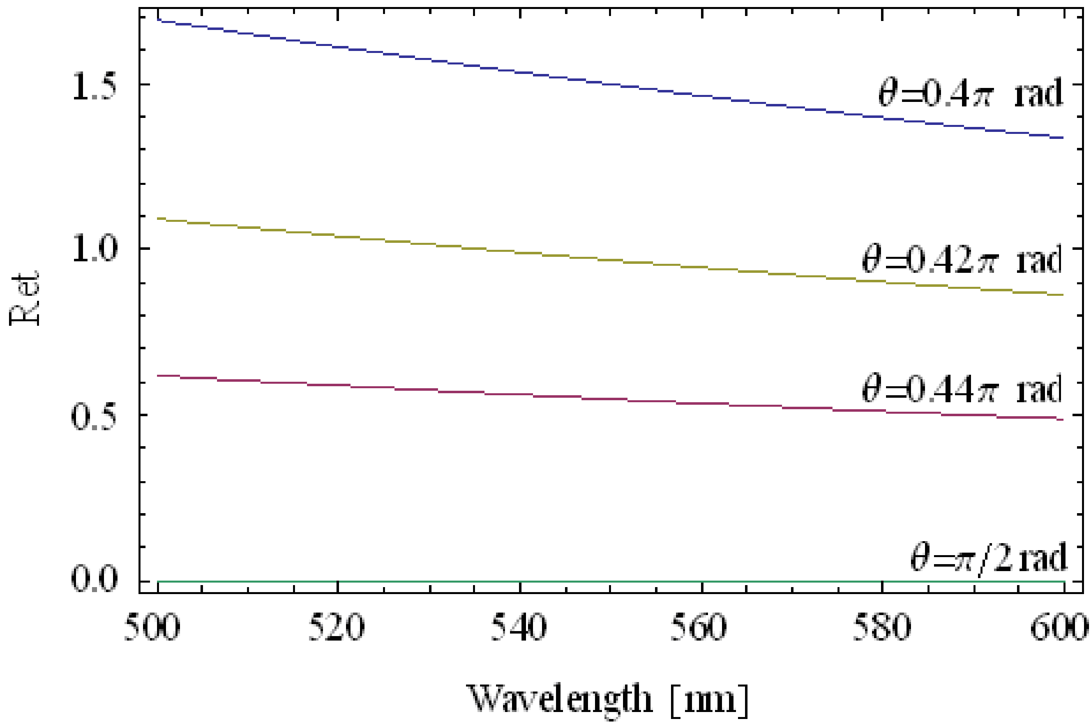

Figure 21 –Plot of effective retardance vs. wavelength for thicknesses of 20 and 100 μm

5. EVALUATION of MODULATION FACTOR

Introducing values:

$$K_{\alpha} = \frac{1}{2}\left\{1 + \frac{1}{\Delta\lambda}\left\{\int_{\lambda_0-\Delta\lambda/2}^{\lambda_0+\Delta\lambda/2} \cos[2\pi\rho_{\alpha}(\vartheta,\lambda)]d\lambda + \int_{\lambda_0-\Delta\lambda/2}^{\lambda_0+\Delta\lambda/2} \sin[2\pi\rho_{\alpha}(\vartheta,\lambda)]d\lambda\right\}\right\} \quad \alpha = 1, 2, 3, 4 \quad (18)$$

Where:

- λ_0 is the central-wavelength;
- $\Delta\lambda$ is the bandwidth;
- $\rho_{\alpha}(\vartheta,\lambda)$ is the equation of retardance (ρ) vs. wavelength (λ), for ϑ (tilt angle) that give retardance values of 0, 0.25, 0.5 and 0.75 waves at λ_0 ($\alpha = 1,2,3,4$ respectively).

We define the modulation factors:

$$\begin{cases} \mu_{+} = \dfrac{K_1 - K_3}{K_1 + K_3} \\ \mu_{-} = \dfrac{K_2 - K_4}{K_2 + K_4} \end{cases} \quad (19)$$

And the average of modulation factors:

$$\mu_{*} = \frac{2}{\sqrt{2}} \frac{\sqrt{(K_1 - K_3)^2 + (K_2 - K_4)^2}}{K_1 + K_2 + K_3 + K_4} \quad (20)$$

At $\lambda_0 = 550nm$, using LCs thicknesses of 10 and 20 μm:

$$\begin{cases} \rho_1 = 0 \;\; \Rightarrow \vartheta = \dfrac{\pi}{2}[rad] \\ \rho_2 = 0.25 \;\; \Rightarrow \vartheta = 1.059[rad] \\ \rho_3 = 0.5 \;\; \Rightarrow \vartheta = 0.790[rad] \\ \rho_4 = 0.75 \;\; \Rightarrow \vartheta = 0.486[rad] \end{cases} \quad (21)$$

Plots of modulation factor μ_{*} vs. bandwidth are shown in Fig. 22. For a 100 nm bandwidth, from 500 to 600nm, we have:

$$\begin{cases} \mu_+ = 0.975 \\ \mu_- = 0.953 \\ \mu_* = 0.964 \end{cases} \quad (22)$$

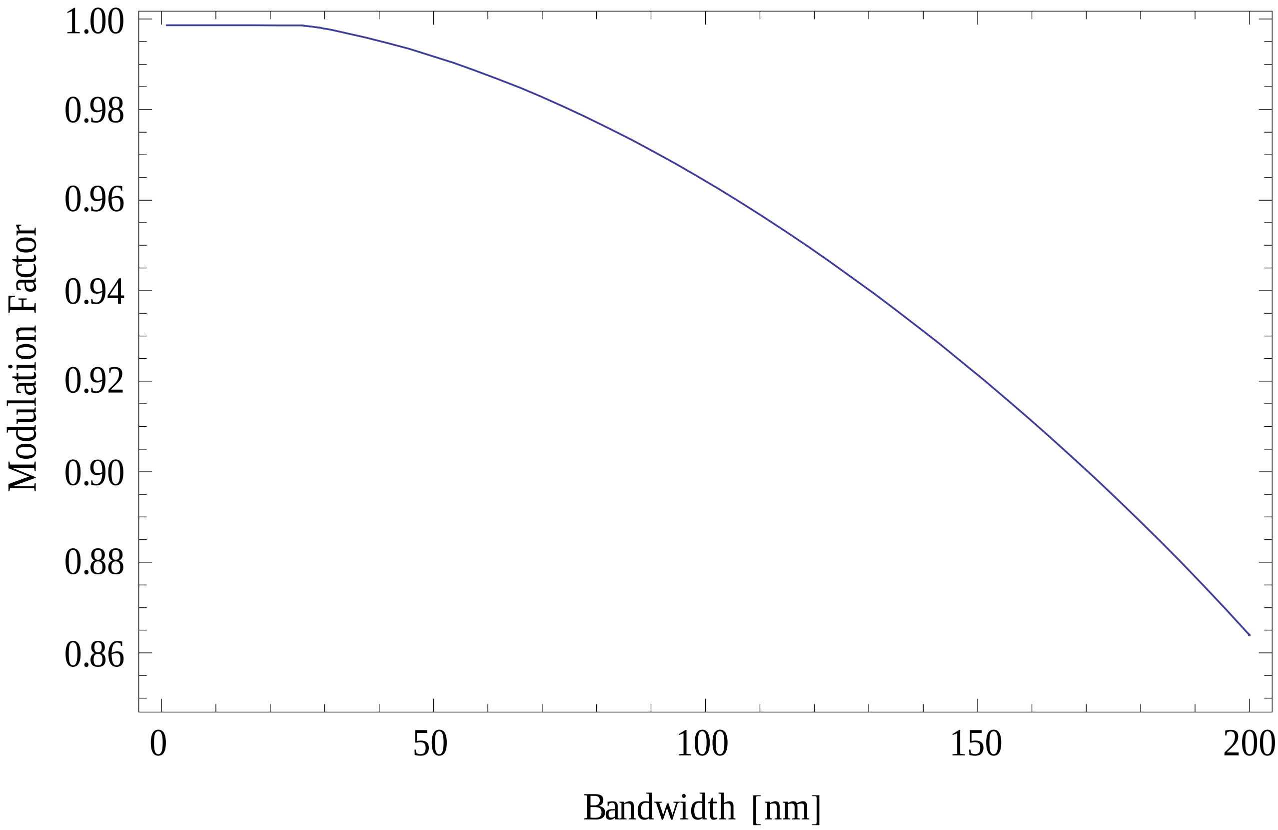

Figure 22 – *Plot of average of modulation factors (μ*) vs. bandwidth for thicknesses of 10 and 20 μm*

Using theoretical thicknesses of 20 and 36 μm and values of tilt angles reported in (23) we obtain the values plotted in Fig.23.

$$\begin{cases} \rho_1 = 0 \quad \Rightarrow \vartheta = \dfrac{\pi}{2}[rad] \\ \rho_2 = 0.25 \quad \Rightarrow \vartheta = 1.09[rad] \\ \rho_3 = 0.5 \quad \Rightarrow \vartheta = 0.82[rad] \\ \rho_4 = 0.75 \quad \Rightarrow \vartheta = 0.42[rad] \end{cases} \quad (23)$$

For a bandwidth of 100 nm:

$$\begin{cases} \mu_+ = 0.970 \\ \mu_- = 0.909 \\ \mu_* = 0.939 \end{cases} \quad (24)$$

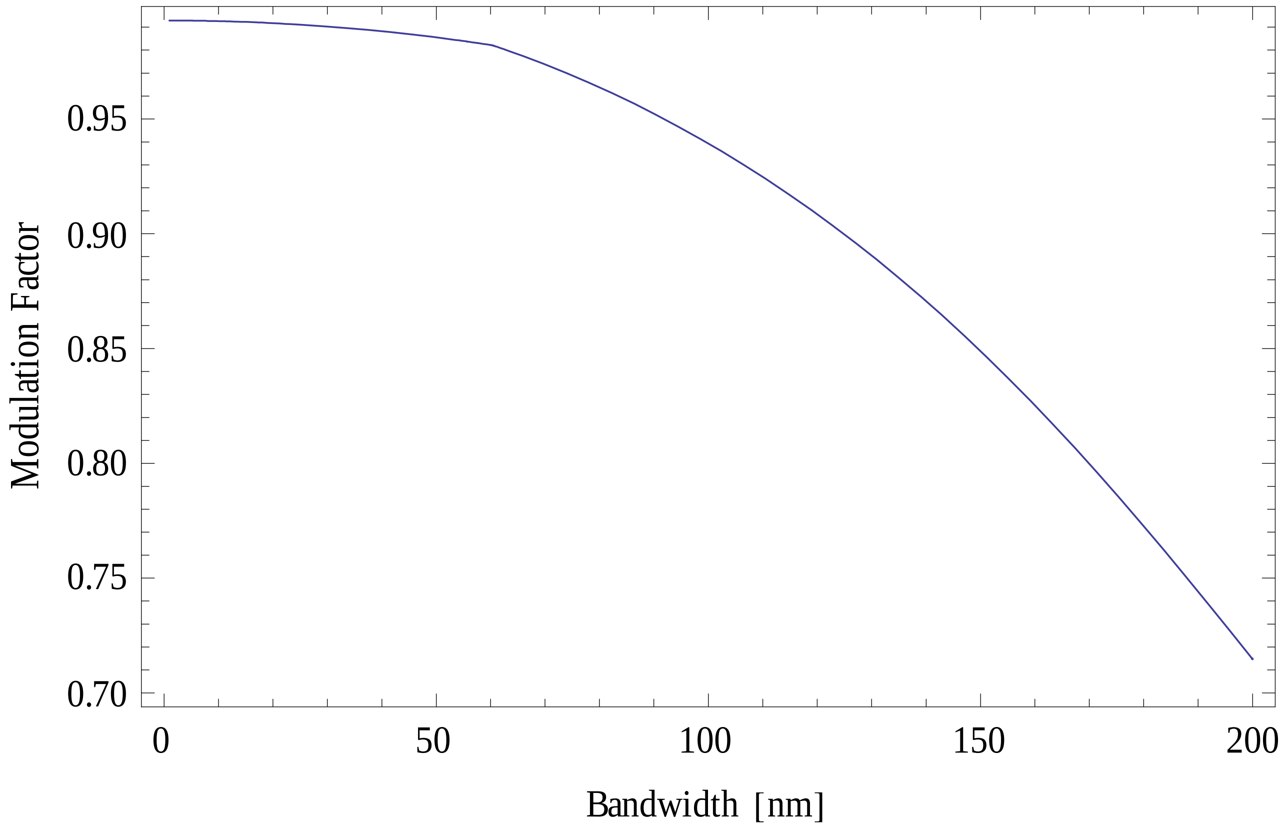

Figure 23 –*Plot of average of modulation factors (μ*) vs. modulation factors vs. bandwidth for thicknesses of 20 and 36 μm*

6. CONCLUSIONS

Resuming:

- Thicknesses of 10 and 20 μm give us maximum chromaticity of 15%, maximum retardance is 0.9 waves and modulation factors are: 0.975 and 0.953 for μ_+ and for μ_- and an average of 0.964 ;
- Ideal thicknesses are 20 and 36 μm that give us retardance of 0.75-wave, maximum chromaticity less than 10% and modulation factors greater than 0.94, but this thicknesses are not commercially.

REFERENCES

[1] Shin-Tson Wu - *Birefringence Dispersions of Liquid Crystals*, Physical Review A Vol.**33** nr .2 (feb. 1986)

[2] Martienssen and Watlimont - *Handbook of condensed matter and materials data* Springer

[3] Li et al. Refractive Indices of Liquid Crystals for Display applications, IEEE/OSA Journal of Display Technology Vol .1 Nr .1 (sept. 2005)

[4] Heynderickx and De Raedt – *Calculation of the director configuration of Nematic liquid crystals by the simulated-anneal method*, Physical Review A Vol. **37** nr. 5 (March 1988)

[5] P. Kohns et al. –*Birefringence measurements of liquid crystals and an application: An achromatic waveplate*, Liquid Crystals Vol. **21** nr. 6 (1996)

[6] L. Vicari, ed. - *Optical Applications of Liquid Crystals*, Series in Optics and Optoelectronics (Institute of Physics, 2003).

[7] N.Uribe-Patarroyo and A.Alvarez-Herrero – *Determination of the molecular tilt profile of a liquid crystal under applied electric field by generalized transmission ellipsometry*, J. Opt. Soc. Am. B Vol. **26** nr. 6 (June 2009)

APPENDIX A – ALCVR Review of the Requirements

Using the same format of [Draft1], the requirements for Achromatic LCVRs are:

Id.	Requirement	Value	Verif.	Comments
F-3	Operational Wavelength	500 – 600 nm	T	Achromatic range for ALCVRs
F-5	Retardation Range	0 - 0.75 λ	T	
F-7	Retardance variation	< 5%	T	In the achromatic range
F-8	Acceptance Angle	± 3 degrees	T	

[Draft1]: Review of the Requirements and technology Review Report LCVR-INTA-TN-001

APPENDIX B – Science Requirements

In the range of wavelength 500 < λ < 600 nm, we want to measure polarization with precision of:

$$\Delta P_{K-Corona} \cong \frac{1}{\mu \cdot SNR} \leq 10^{-2} \qquad \text{(B.1)}$$

Where μ is the modulation factor and SNR is the signal to noise ratio.

The polarization of K-Corona is of order of:

$$P_{K-Corona} \approx 10^{-1} \qquad \text{(B.2)}$$

Than, assuming $\mu \approx 1$, we obtain:

$$\Delta\mu \approx 10^{-2} \qquad \text{(B.3)}$$

For small departure from the achromatism, the Taylor expansion of Eq. 18:

$$K_\alpha \cong \frac{1}{2}\left\{1+\left[1-\frac{1}{2}(2\pi\Delta\rho)^2+2\pi\Delta\rho\right]\right\} \qquad \text{(B.4)}$$

we obtain the following rule of thumb:

$$\Delta\mu \approx \frac{1}{2}(2\pi\ \Delta\rho)^2 \qquad \text{(B.5)}$$

Where ρ is the retardance.

From B.4 and B.3, we obtain:

$$\Delta\rho \approx 10^{-1} \qquad \text{(B.6)}$$

This result is in good agreement with the numerical simulation and results resumed in section 6 of this document.